J|A|C|S
ARTICLES
Published on Web 03/22/2002

A Mechanism from Quantum Chemical Studies for Methane Formation in Methanogenesis

Vladimir Pelmenschikov,[†] Margareta R. A. Blomberg,[†] Per E. M. Siegbahn,*[,†] and Robert H. Crabtree[‡]

Contribution from the Department of Physics, Stockholm University, Box 6730, S-113 85 Stockholm, Sweden, and Chemistry Department, Yale University, P.O. Box 208107, 225 Prospect Street, New Haven Connecticut 06520-8107

Received July 9, 2001. Revised Manuscript Received November 21, 2001

Abstract: The mechanism for methane formation in methyl-coenzyme M reductase (MCR) has been investigated using the B3LYP hybrid density functional method and chemical models consisting of 107 atoms. The experimental X-ray crystal structure of the enzyme in the inactive $MCR_{ox1-silent}$ state was used to set up the initial model structure. The calculations suggest a mechanism not previously proposed, in which the most remarkable feature is the formation of an essentially free methyl radical at the transition state. The reaction cycle suggested starts from a Michaelis complex with CoB and methyl-CoM coenzymes bound and with a squareplanar coordination of the Ni(I) center in the tetrapyrrole F_{430} prosthetic group. In the rate-limiting step the methyl radical is released from methyl-CoM, induced by the attack of Ni(I) on the methyl-CoM thioether sulfur. In this step, the metal center is oxidized from Ni(I) to Ni(II). The resulting methyl radical is rapidly quenched by hydrogen-atom transfer from the CoB thiol group, yielding the methane molecule and the CoB radical. The estimated activation energy is around 20 kcal/mol, which includes a significant contribution from entropy due to the formation of the free methyl. The mechanism implies an inversion of configuration at the reactive carbon. The size of the inversion barrier is used to explain the fact that $CF_3-S-CoM$ is an inactive substrate. Heterodisulfide $CoB-S-S-CoM$ formation is proposed in the final step in which nickel is reduced back to Ni(I). The suggested mechanism agrees well with experimental observations.

I. Introduction

Archaebacteria (*Archaea*) contain several nickel enzymes, a metal otherwise rather rare in biochemistry.[1,2] In several cases, such as CO dehydrogenase, the nickel is generally assumed to form organometallic intermediates—ones with a direct Ni−C bond.[1] Methanogenic bacteria are a diverse subgroup of archaebacteria that use methane formation to provide energy for the cell.[3] One such pathway, shown in eq 1, involves the release of 31 kcal/mol,

$$CO_2 + 4H_2 \rightarrow CH_4 + 2H_2O \qquad (1)$$

In this case, the overall $8e^-$ reduction of CO_2 occurs via four $2e^-$ steps, the reduced carbon fragment being bound to a series of coenzymes. This report is concerned only with the final step, in which two coenzymes are involved: one, coenzyme M, carries the methyl group that comes from CO_2 reduction and the other, coenzyme B, is an aliphatic thiol. This last step, represented by eq 2, is a topic of intense current interest.[4,5]

$$CoB-S-H + CH_3-S-CoM \rightarrow CoB-S-S-CoM + CH_4 \qquad (2)$$

Catalyzed by the nickel-dependent protein, methylcoenzyme M reductase (MCR), the reaction in eq 2 involves the release of 11 kcal/mol[6,7] and occurs in the oxidative part of the methanogenic archaea energy metabolism. The heterodisulfide also formed is subsequently hydrogenolyzed with H_2 back to the thiol forms of the separate cofactors by heterodisulfide reductase[8,10] in the reductive part of the cycle.

The key MCR enzyme has an $\alpha_2\beta_2\gamma_2$ subunit structure and, as normally isolated, contains two molecules of a nickel porphyrinoid cofactor, denoted F_{430} because of its absorption maximum at 430 nm, along with two molecules each of

* To whom correspondence should be addressed. E-mail: ps@physto.se.
[†] Stockholm University.
[‡] Yale University.

(1) Ragsdale, S. W. *Curr. Opin. Chem. Biol.* **1998**, *2*, 208−215.
(2) Ermler, U.; Grabarse, W.; Shima, S.; Goubeard, M.; Thauer, R. K. *Curr. Opin. Struct. Biol.* **1998**, *8*, 749−758.
(3) Thauer, R. K. *Microbiology* **1998**, *144*, 2377.
(4) Cammack, R. *Nature* **1997**, *390*, 443.
(5) Ferry, J. G. *Science* **1997**, *278*, 1413.
(6) Thauer, R. K.; Hedderich, R.; Fischer, R. In *Methanogenesis*; Ferry, J. G., Ed.; Chapman and Hall: New York and London, 1993; Chapter 2, p 209.
(7) Becker, D. F.; Ragsdale, S. W. *Biochemistry* **1998**, *37*, 2639.
(8) Heiden, S.; Hedderich, R.; Setzke, E.; Thauer, R. K. *Eur. J. Biochem.* **1993**, *213*, 529.
(9) Ermler, U.; Grabarse, W.; Shima, S.; Goubeard, M.; Thauer, R. K. *Science* **1997**, *278*, 1457.
(10) Setzke, E.; Hedderich, R.; Heiden, S.; Thauer, R. K. *Eur. J. Biochem.* **1994**, *220*, 139.

10.1021/ja011664r CCC: $22.00

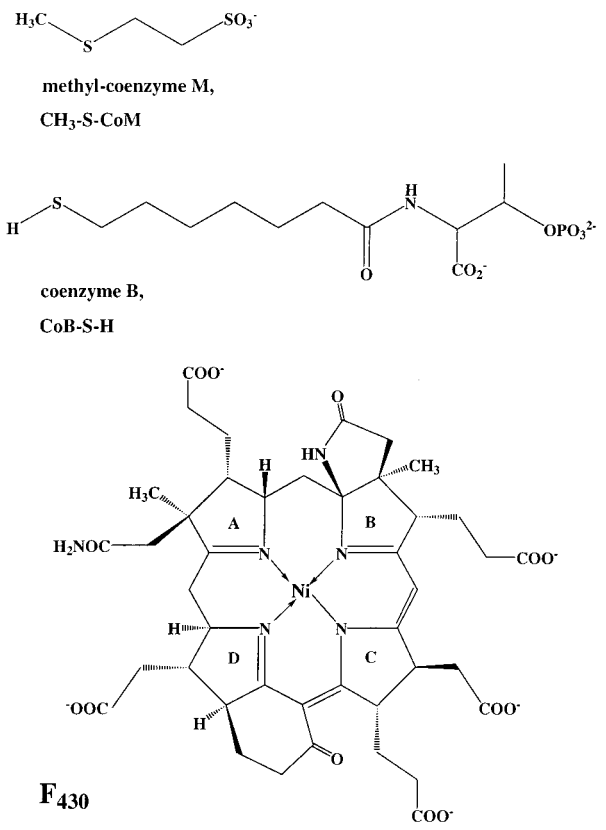

Figure 1. Structures of methyl-coenzyme M, coenzyme B, and F_{430} prosthetic group, required for methane formation in methanogens.

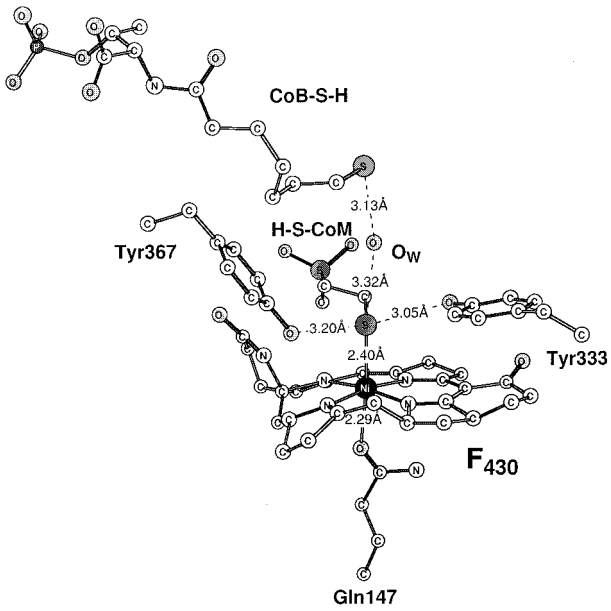

Figure 2. Active site region of methyl-coenzyme M reductase as found in the X-ray structure of the enzyme in the $MCR_{ox1-silent}$ state.[9] Peripheral substituents of the F_{430} prosthetic group are omitted for clarity.

coenzymes B and M. The structures of these cofactors are shown in Figure 1. See also Figure 2.

In the Ni(II) state, F_{430} can be four- or six-coordinate, and can be readily reduced to a Ni(I) form. Unlike true porphyrins, which have a Ni(II) center and a reduced porphyrin, F_{430} contains authentic Ni(I), as shown by the EPR spectrum.[11] Ni(I) is believed to be relevant to the mechanism because the enzyme only becomes active when the resting Ni(II) state of F_{430} is reduced to Ni(I), for example with Ti(III) salts.[12]

Methyl-coenzyme M (2-mercaptoethanesulfonic acid) has the simplest cofactor structure known and is unique to the methanogens. Coenzyme B (7-mercaptoheptanoylthreonine phosphate) has an aliphatic linker of six methylene units between the phosphothreonine headgroup and the thiol group. Alteration in the length of this linker is very deleterious to activity. Having one less methylene gives only 1% of activity, and having one more methylene abolishes activity completely.[13]

Some insight into the reason for the sensitivity to linker length comes from the crystal structure of the protein from *Methanobacterium thermoautotrophicum*.[9] Two independent active sites are located 50 Å apart. Each consists of a nonpolar pit 30 Å deep and about 6 Å in diameter. F_{430} is located at the bottom of the pit. Hanging down from the top is coenzyme B, anchored at the top by salt bridges involving surface residues and the phosphothreonine headgroup that lies at and partially blocks the mouth of the pit. The six methylenes of the linker allow the CoB sulfur atom to hang 8.7 Å above the Ni atom of F_{430}. Between CoB and Ni lies the small CoM cofactor. In the particular state studied, the CoM sulfur is bound to the Ni.

In view of the presence of Ni−C bonds in other Ni enzymes and of Co−C bonds in many derivatives of the well-known and somewhat related coenzyme B_{12}, it was perhaps inevitable that the mechanisms suggested for methanogenesis have all involved formation of a $Ni-CH_3$ bond at some point, usually followed by protonolysis to release methane.[3] One of the mechanisms proposed in ref 3 is illustrated in Figure 3 and summarized in the set of eqs 3−5. The first step is suggested to be a methyl cation transfer from methyl-CoM to nickel, yielding a $CH_3-Ni(III)F_{430}^+$ compound. It is further assumed that this heterolytic cleavage of the *S*-methyl bond needs to be accompanied by a proton transfer to the CoM-leaving group, and that a possible source for the proton could be CoB. This first step can then be summarized in eq 3:

$$CoB-S-H + CH_3-S-CoM + Ni(I)F_{430} \rightarrow CoB-S^- + H-S-CoM + CH_3-Ni(III)F_{430}^+ \quad (3)$$

Thus, apart from cleaving the $S-CH_3$ bond and forming the Ni−C bond, this step also includes a charge separation. The $CH_3-Ni(III)F_{430}^+$ compound is a strong oxidant, and in the next step it is suggested to oxidize H−S−CoM yielding a cation radical on CoM according to eq 4:

$$H-S-CoM + CH_3-Ni(III)F_{430}^+ \rightarrow H-{}^{\bullet}S-CoM^+ + CH_3-Ni(II)F_{430} \quad (4)$$

$CH_3-Ni(II)F_{430}$ is suggested to be spontaneously protonolyzed to give CH_4 and $Ni(II)F_{430}^+$, using the proton of the CoM thiyl radical cation. The CoM thiyl radical and the CoB thiolate are assumed to combine into $CoB-S-{\bullet}S-CoM^-$ disulfide radical anion, which reduces Ni(II), forming the final neutral products

(11) Pfaltz, A. In *The Bioinorganic Chemistry of Nickel*; Lancaster, J. R., Ed.; VCH: Weinheim, 1988; Chapter 12.
(12) Goubeaud, M.; Schreiner, G.; Thauer, R. K. *Eur. J. Biochem.* **1997**, *243*, 110.
(13) Ellermann, J.; Hedderich, R.; Boecher, R.; Thauer, R. K. *Eur. J. Biochem.* **1988**, *172*, 669.

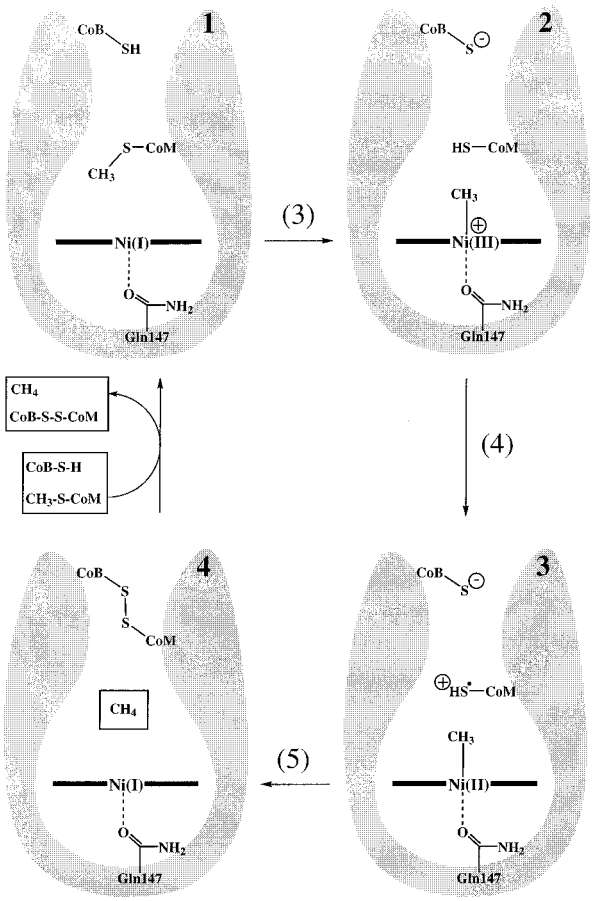

Figure 3. Sketch of a previously suggested mechanism for methyl-CoM reductase.[9] The Ni−CH_3 bond formed at point **2** is subsequently protonolyzed to form methane when proceeding from **3** to **4**.

and closing the reaction cycle. The last step thus can be given as eq 5:

$$\mathrm{CoB{-}S^- + H{-}{}^{\bullet}S{-}CoM^+ + CH_3{-}Ni(II)F_{430} \rightarrow CoB{-}S{-}S{-}CoM + CH_4 + Ni(I)F_{430}} \quad (5)$$

When methane and the disulfide have left the active-site cleft, the enzyme is ready for the next cycle. As will be discussed below, the present calculations indicate that the nickel−methyl bond strength is too low to make this reaction scheme energetically plausible.

In an alternative mechanism, also described in ref 3, methyl-CoM is proposed to be activated by a CoB thiyl radical, such that a homolytic cleavage of the methyl−S bond is favored, directly yielding a CH_3−Ni(II)F_{430} compound. This mechanism thus assumes the presence of a strong oxidant, capable of oxidizing CoB into a thiyl radical. However, the only redox center at the active site of methyl-coenzyme M reductase is Ni(II)F_{430}, but this center has been experimentally ruled out as the oxidant.

The present contribution uses DFT methods to examine possible mechanisms with the very unexpected result that Ni−C bonded intermediates can be excluded and the proposed mechanism involves a nickel-induced release of •CH_3 radical from CH_3−S−CoM that is immediately quenched by H-atom transfer from CoB−S−H.

II. Computational Details

The calculations were performed in two steps. For each structure considered, a full geometry optimization was performed using the hybrid density functional B3LYP method.[14,15] In this first step, standard double-ζ basis sets were used for all light elements. For nickel a nonrelativistic Hay and Wadt[16] effective core potential (ECP) was used. The valence basis set used in connection with this ECP is essentially of double-ζ quality. The geometry optimizations were carried out with either the GAUSSIAN program[17,18] using the *lanl2dz* basis or the Jaguar 4.0 program[19] using the *lacvp* basis. The GAUSSIAN program and the *lanl2dz* basis was used also for the Hessian calculations, that is, the second derivatives of the energy with respect to the nuclear coordinates. Some restrictions, taken from the X-ray structure, were superimposed on the geometry optimizations, as further described in the text below. In a second step, the energy was evaluated for the optimized geometries using larger basis sets of triple-ζ quality in the valence region, and including a single set of polarization functions on each atom. This final energy evaluation was performed at the B3LYP level using the Jaguar 4.0 program and the *lacv3p*** basis. The inherent accuracy of the B3LYP method can be estimated from benchmark tests, in which the average error in the atomization energies for 55 small first- and second-row molecules is found to be 2.2 kcal/mol.[20] For transition metals there are no benchmarks due to the lack of accurate experimental numbers but indications from normal metal−ligand bond strengths are that the errors are slightly larger, 3−5 kcal/mol.[21]

The surrounding protein was treated using self-consistent reaction field methods, where the cavity follows the shape of the molecular system. For Jaguar, a Poisson−Boltzmann solver was used with a probe radius of 1.40 Å corresponding to the water molecule, while for Gaussian, the conductor-like polarized continuum model (CPCM, or COSMO) method[22] was used, again with water as a probe. The dielectric constant of the protein is the main empirical parameter of these methods, and it was chosen to be equal to 4 in line with previous suggestions for proteins. In agreement with previous findings the calculated dielectric effects on the relative energies were found to be small for reactions where the charge state of the model is constant.

The relative energies discussed below are those obtained using the large *lacv3p*** basis set, while zero-point vibrational effects, entropy effects, and dielectric effects are included only when specifically stated.

(14) Becke, A. D. *Phys. Rev.* **1988**, *A38*, 3098; Becke A. D. *J. Chem. Phys.* **1993**, *98*, 1372; Becke, A. D. *J. Chem. Phys.* **1993** *98*, 5648.
(15) Stevens, P. J.; Devlin, F. J.; Chablowski, C. F.; Frisch, M. J. *J. Phys. Chem.* **1994**, *98*, 11623.
(16) Hay, P. J.; Wadt, W. R. *J. Chem. Phys.* **1985**, *82*, 299.
(17) Frisch, M. J.; Trucks, G. W.; Schlegel, H. B.; Gill, P. M. W.; Johnson, B. G.; Robb, M. A.; Cheeseman, J. R.; Keith, T.; Petersson, G. A.; Montgomery, J. A.; Raghavachari, K.; Al-Laham, M. A.; Zakrzewski, V. G.; Ortiz, J. V.; Foresman, J. B.; Cioslowski, J.; Stefanov, B. B.; Nanayakkara, A.; Challacombe, M.; Peng, C. Y.; Ayala, P. Y.; Chen, W.; Wong, M. W.; Andres, J. L.; Replogle, E. S.; Gomperts, R.; Martin, R. L.; Fox, D. J.; Binkley, J. S.; Defrees, D. J.; Baker, J.; Stewart, J. P.; Head-Gordon, M.; Gonzalez, C.; Pople, J. A. *Gaussian 94*, Revision B.2; Gaussian Inc.: Pittsburgh, PA, 1995.
(18) Frisch, M. J.; Trucks, G. W.; Schlegel, H. B.; Scuseria, G. E.; Robb, M. A.; Cheeseman, J. R.; Zakrzewski, V. G.; Montgomery, J. A., Jr.; Stratmann, R. E.; Burant, J. C.; Dapprich, S.; Millan, J. M.; Daniels, A. D.; Kudin, K. N.; Strain, M. C.; Farkas, O.; Tomasi, J.; Barone, V.; Cossi, M.; Cammi, R.; Mennucci, B.; Pomelli, C.; Adamo, C.; Clifford, S.; Ochterski, J.; Petersson, G. A.; Ayala, P. Y.; Cui, Q.; Morokuma, K.; Malick, D. K.; Rabuck, A. D.; Raghavachari, K.; Foresman, J. B.; Cioslowski, J.; Ortiz, J. V.; Stefanov, B. B.; Liu, G.; Liashenko, A.; Piskorz, P.; Komaromi, I.; Gomperts, R.; Martin, R. L.; Fox, D. J.; Keith, T.; Al-Laham, M. A.; Peng, C. Y.; Nanayakkara, A.; Gonzalez, C.; Challacombe, M.; Gill, P. M. W.; Johnson, B.; Chen, W.; Wong, M. W.; Andres, J. L.; Head-Gordon, M.; Replogle, E. S.; Pople, J. A. *Gaussian 98*; Gaussian Inc.: Pittsburgh, PA, 1998.
(19) Jaguar 4.0, Schrödinger, Inc., Portland, OR, 1991−2000.
(20) Bauschlicher, C. W., Jr.; Ricca, A.; Partridge, H.; Langhoff, S. R. In *Recent Advances in Density Functional Methods, Part II*; Chong, D. P., Ed.; World Scientific Publishing Company: Singapore, 1997; p 165.
(21) Siegbahn, P. E. M.; Blomberg, M. R. A. *Annu. Rev. Phys. Chem.* **1999**, *50*, 221−249.
(22) Barone, V.; Cossi, M. *J. Phys. Chem.* **1998**, *102*, 1995−2000.

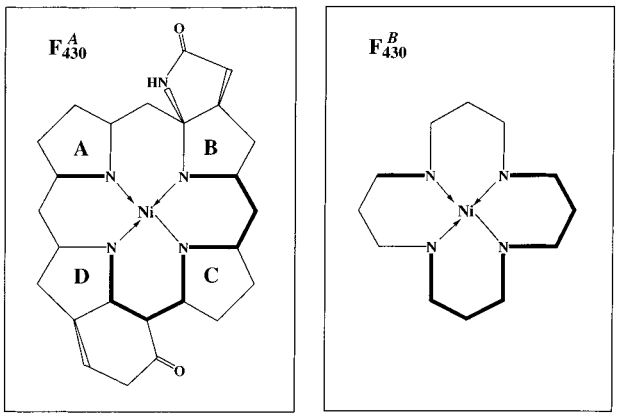

Figure 4. Two different nickel complexes used to model the F_{430} cofactor. Conjugated areas or double bonds of the tetrapyrrole are shown in bold.

III. Results and Disscusion

The first step in every theoretical study of an enzyme mechanism is to choose a chemical model that describes the active site reasonably well yet is not too large and therefore impractical. In the present case useful models have to be selected for the F_{430}, CoM and CoB cofactors. Finally, important additional hydrogen bonds have to be identified. These modeling considerations are discussed in section III.a. below. The next step in the present study was to calculate some key bond strengths. In particular, from the experimentally suggested mechanisms described above, it is clear that the Ni−CH_3 bond strengths for both Ni(II) and Ni(III) are critical quantities. These and other bond strengths are discussed in section III.b. The bond strengths obtained combined with key experimental information, suggests a quite different mechanism from the ones proposed earlier. This new mechanism is discussed in section III.c. In section III.d., the calculations using the largest model are described and in section III.e. the implication of stereoinversion at the reactive carbon are discussed. Finally, the electronic and geometric structure of the F_{430} cofactor are described.

III.a. Chemical Models. The present modeling study is based on the experimentally determined structure of the methyl-coenzyme reductase in the $MCR_{ox1-silent}$ state. Two different models for the F_{430} tetrapyrrole cofactor were tested, see Figure 4. The largest one, F_{430}^{A}, includes four pyrrole rings of the cofactor, a lactam ring joined with pyrrole B, and a six-membered carbocyclic ring joined with pyrrole D. The propionate substituents of the rings A, B, and C, and acetate substituents of C and D, anchoring F_{430} by the carboxylate groups to the protein, were replaced by hydrogens. The methyl groups at A and B, and the acetamide substituent of A were also omitted to reduce the size of the system and to make it computationally feasible. The less extended model used at the initial stage of our investigations is a Ni-chelating macrocycle complex F_{430}^{B}, where the pyrrole rings are broken. The F_{430} cofactor is the most saturated tetrapyrrole known in nature. The low degree of conjugation supports the use of less extended models such as F_{430}^{B}, where the existing conjugation of the original cofactor is retained. For the catalytic properties of the nickel center, the difference between the F_{430}^{A} and F_{430}^{B} models was found to be quite small, see further below in the text. The F_{430} prosthetic group is known to be extremely flexible, again due to the absence of extensive conjugation. To better model the F_{430} deformations, important for the heterodisulfide formation (not discussed in the present report), the F_{430}^{A} model is perhaps better than F_{430}^{B} which may be somewhat less flexible.

The most critical properties of methyl-coenzyme M that need to be accurately modeled are the CH_3-SCoM and the Ni−SCoM bond strengths. The CH_3-SCoM bond strength, as given by reaction 7,

$$CH_3\bullet + \bullet S-CoM \rightarrow CH_3-S-CoM \qquad (7)$$

turns out to be surprisingly insensitive to the size of the model. The simplest possible model, CH_3-S-CH_3, and the full model of this cofactor, including also the terminal sulfonate group that anchors the cofactor to the polypeptide chain in the wall of the pit, give very similar bond strengths of 70.1 and 69.8 kcal/mol, respectively. When other substrates were investigated, see section III.e., it was found that even the $S-CHF_2$ and $S-CF_3$ bond strengths are very similar to that of methyl, and independent of the size of the cofactor model. The bond strength between sulfur and nickel, as given by reaction 8,

$$CoM-S\bullet + Ni(I)F_{430} \rightarrow CoM-S-Ni(II)F_{430} \qquad (8)$$

is more difficult to estimate. The reason is that it is difficult to describe the hydrogen-bonding interactions in a balanced way before and after the formation of the Ni−S bond. However, when the smallest possible model of methyl-coenzyme M, CH_3-S-CH_3, is used, a good approximation should be to neglect the additional hydrogen bonding. In that case a Ni−S bond strength of 38.6 kcal/mol is obtained using the F_{430}^{B} model for the nickel cofactor. In another model the entire coenzyme M was used explicitly, including its sulfonate group. The sulfonate was protonated since its negative charge should be balanced by a salt bridge to the guanidium group of Arg120 and by two hydrogen bonds to the peptide nitrogen of Tyr444 and His364, as indicated by the X-ray structure.[9] The full model of coenzyme M, gives a reaction energy for reaction 8 of 46.1 kcal/mol. A major part of the difference from the small model is the unbalanced hydrogen-bonding energy. For this reason, the most realistic value for the Ni−S bond strength should come from the use of the small coenzyme M model of 38.6 kcal/mol. Still, in the final calculations of the mechanism described below, methyl-coenzyme M was modeled explicitly, including the sulfonate group, since this is inherently a better model, and the above problem in describing reaction 8 does not occur for the full reaction. In modeling coenzyme B, the heptanoyl arm can be simplified to an ethanethiol CH_3CH_2-S-H, or even a methanethiol, without significant loss of accuracy.

The Gln147 on the rear face of F_{430}, which binds to the Ni center with its side-chain oxygen with a bond distance of 2.3 Å in the X-ray structure, was modeled by an acetamide molecule for the large F_{430}^{A} model, and by a formamide molecule for the smaller F_{430}^{B} model. Among the other amino acids close to the active site, only the two tyrosines, Tyr333 and Tyr367, were included in view of the mechanism proposed. Interacting by their hydroxyl groups with the coenzyme M sulfur, the tyrosines were modeled by methanols, which should be quite sufficient for describing just the hydrogen bonds to sulfur.

III.b. The Binding of Methyl to Nickel. A key part of the previously suggested mechanisms, shown in Figure 3 and described in the Introduction, is the binding of methyl to nickel.

Methyl is bound to nickel in the Ni(III) state at point **2** and in the Ni(II) state at point **3**. A first test of this mechanism is therefore to calculate these bond strengths. A binding energy of methyl to the $Ni(I)F_{430}^{B}$ complex of only 24.9 kcal/mol was obtained using the large basis set, following eq 9 with infinitely separated reactants:

$$CH_3\bullet + Ni(I)F_{430} \rightarrow CH_3{-}Ni(II)F_{430} \quad (9)$$

For the methyl binding to the positively charged $Ni(II)F_{430}^{B+}$ complex as given in eq 10:

$$CH_3\bullet + Ni(II)F_{430}^{+} \rightarrow CH_3{-}Ni(III)F_{430}^{+} \quad (10)$$

an even smaller energy of 18.0 kcal/mol was found. Therefore, for the methyl transfer from methyl-CoM to Ni as given in eq 11:

$$CH_3{-}S{-}CoM + Ni(I)F_{430} \rightarrow \bullet S{-}CoM + CH_3{-}Ni(II)F_{430} \quad (11)$$

to be energetically possible, the binding energy of methyl to sulfur in methyl-coenzyme M have to be not much greater than 25 kcal/mol. In other words, reaction 11 will be endothermic by at least the amount that the $S{-}CH_3$ bond strength in methyl-coenzyme M is larger than the $Ni(II){-}CH_3$ bond strength. As already mentioned in the previous section, the $S{-}CH_3$ bond strength in methyl-coenzyme M is quite insensitive to the modeling of the cofactor. For the full cofactor the bond strength is found to be 69.8 kcal/mol, while for the simple $S(CH_3)_2$ model it is 70.1 kcal/mol. Thus, the process in eq 11 would be endothermic by about 45 kcal/mol.

The products of the second step in the previously proposed mechanism (right side of eq 4, or point **3** in Figure 3) differ from the products in eq 11 by a proton transfer between the cofactors as given in eq 12:

$$CoB{-}S{-}H + \bullet S{-}CoM \rightarrow CoB{-}S^{-} + H{-}{}^{\bullet}S{-}CoM^{+} \quad (12)$$

For the minimal methyl models of CoM and CoB, the step in eq 12 was found to be endothermic by 67.3 kcal/mol for the infinitely separated compounds. The surrounding protein was treated as described in section II. Including the Coulombic attraction between the $CoB{-}S^{-}$ thiolate and $\bullet SH{-}CoM^{+}$ thiyl radical cation at 8.7 Å leads to a decrease of this very large value down to 53.9 kcal/mol. Combining reactions 11 and 12, this means that point **3** in Figure 3 is predicted to be as much as 100 kcal/mol higher than the initial reactants in point **1** using the best present models. Considering probable stabilizing effects from the particular groups in the MCR active site cannot bring this large value down to a kinetically feasible one. Unless B3LYP has a very large error, very unlikely on the basis of previous benchmark tests,[23,24] this result rules out the mechanism shown in Figure 3. The capability of Ni(III) in F_{430} to oxidize the CoM thiol group appears to have been overestimated, since reaction 4 of the CoM thiyl radical formation is highly endothermic by 73 kcal/mol, including the protein-surrounding effects and charge-separation estimates.

A few additional results obtained when the above bond strengths were calculated have implications for the mechanism and modeling of the methane formation reactions. First, testing different spin-states for the $Ni(II){-}CH_3$ complex, showed quite clearly that the alkyl is predicted to have a triplet ground state. This is not so surprising since for this complex a strong bond to methyl (ionic or covalent) has to be formed perpendicular to the tetrapyrrole ring. Singlet Ni(II) forms strong bonds only in one plane, while triplet Ni(II) prefers a tetrahedral coordination and is therefore more flexible in forming bonds both in the plane of the tetrapyrrole ring and perpendicular to it. For the same reason, the $Ni(II){-}S{-}CH_3$ complex also has a triplet ground state. Another useful result is that the smaller F_{430}^{B} model gives results very similar to the larger F_{430}^{A} model. The binding of methyl for the Ni(II) state is 21.3 kcal/mol for the larger model using the *lacvp* basis set, differing by only 0.9 kcal/mol from the smaller model with the same basis set. Further comparisons between the models, also showing very good agreement, will be described below. These results show that the smaller model, which leads to significantly faster calculations, can be confidently used to explore different mechanisms.

III.c. A New Mechanism for Methane Formation. From the results discussed in the previous section concerning the bond strength between methyl and nickel, any mechanism requiring a strong bond of this type can be ruled out. The alternative mechanism suggested, where weaker $Ni{-}CH_3$ bonds are allowed, involve the presence of a strong oxidant capable of oxidizing $CoB{-}S{-}H$ into a thiyl radical prior to the methane formation reaction. This would clearly introduce an additional amount of energy sufficient to make the methane formation possible. However, since there is no evidence for such an oxidant, this type of mechanism remains highly speculative. Furthermore, since Ni(I) is the experimentally known active state, the thiyl radical is required to be stable in the presence of Ni(I), which is also very unlikely. It would therefore be advantageous at this stage if another mechanism could be suggested that does not require the action of an additional strong oxidant. On the basis of the present calculations and key experimental information, such a mechanism will be discussed in this section.

Since a transfer of the methyl from methyl-coenzyme M to nickel is now ruled out, the remaining possibility is to transfer the methyl group directly between the cofactors M and B. A puzzle in this context is that the distance between the sulfurs of these cofactors is very long, 6.2 Å, which appears to make a concerted transfer of methyl between the cofactors unlikely. It is also known that cofactor B is firmly bound by several strong hydrogen bonds and is therefore relatively immobile. The coenzyme M sulfur should also become fairly strongly bound to nickel in the process of forming methane, which leads to a rather rigid system where the S···S distance probably cannot be significantly shortened without energy loss.

As a first test of a mechanism where methyl is transferred from methyl-coenzyme M to cofactor B, the energy for releasing a methyl radical can be calculated following reaction 13:

$$CH_3{-}S{-}CoM + Ni(I)F_{430} \rightarrow \bullet CH_3 + CoM{-}S{-}Ni(II)F_{430} \quad (13)$$

Cofactor B is thus left out of the model for the moment. A reliable estimate of this reaction energy is difficult to obtain,

(23) Curtiss, L. A.; Raghavachari, K.; Redfern, R. C.; Pople, J. A. *J. Chem. Phys.* **2000**, *112*, 7374−7383.
(24) Siegbahn, P. E. M.; Blomberg, M. R. A. *Chem. Rev.* **2000**, *100*, 421−437.

since the interaction between the reactants leads to conformers of the cofactors that are unreasonable in the enzyme. However, with the smallest model of methyl-coenzyme M, CH_3-S-CH_3, it is probably not unreasonable to neglect the interaction energy between the reactants. If this is done the reaction energy for reaction 13 will be equal to the difference in the bond strengths described by reactions 7 and 8. Reaction 7 gives the bond strength of methyl to coenzyme M which is 70.1 kcal/mol using the smallest coenzyme M model. Reaction 8 describes the bond strength between the coenzyme M radical (after methyl has departed) and the nickel cofactor. Again, using the smallest coenzyme M model and F_{430}^{B} this bond strength is 38.6 kcal/mol. This means that the energy required to entirely release a methyl radical from coenzyme M according to reaction 13 is estimated to be 32.5 kcal/mol. Although this energy is still too high to be viable thermally, it is approaching values where this mechanism with minor modifications might be feasible.

The energy required for releasing the methyl radical from coenzyme M is thus still rather high using the above very simple models. The question is whether there is anything at the enzyme active site that can be expected to lower this energy further. Indeed, the structure of the enzyme in Figure 2, shows that two tyrosines, Tyr333 and Tyr367, are positioned in a way that can be expected to stabilize the negative sulfur of coenzyme M once the methyl radical has been released. Calculations, where the hydrogen bonding from the two tyrosines are modeled using methanols, lead to a further stabilization of the methyl radical product by 6.6 kcal/mol using the smaller F_{430}^{B} model. This leads to a very plausible role for these tyrosines in the methane formation mechanism. The energy for releasing the methyl radical is now 25.9 (= 32.5 − 6.6) kcal/mol.

The above estimate of 26 kcal/mol for the binding energy of methyl does not contain zero-point and entropy effects, which are expected to further lower this energy. Since the full model of reaction 13 is too large for a calculation of a Hessian, and it was not possible to design a meaningful model small enough to allow for a Hessian calculation, these energies were estimated on the basis of simpler reactions. The simplest of these is the reverse of reaction 7 where the S−C bond is cleaved into radicals. The zero-point energy decrease when this bond is cleaved is 5.6 kcal/mol and the entropy increase is as high as 9.3 kcal/mol. Both these effects go in the direction of lowering the energy required for methyl release in reaction 13. However, these estimates are likely to be too large. The estimated zero-point effect neglects the binding between sulfur and nickel, which is stronger in the product of reaction 13, and the estimated entropy effect exaggerates the free character of the methyl radical at the transition state for methane formation. To obtain a different estimate, the transition state for the following reaction 14 was obtained, see Figure 5,

$$CH_3-S-H + CH_3-S-CH_3 + Na \rightarrow CH_3-S\bullet + CH_4 + CH_3-S-Na \quad (14)$$

in which the Na atom is a model for nickel in reaction 13. From the structures of the reactants and transition state for this reaction, the zero-point effect is found to be −2.6 kcal/mol and the entropy effect −3.8 kcal/mol. While this may be a useful estimate of the zero-point effect it could be argued that the entropy effect is too low due to the harmonic approximation employed, which could underestimate the free character of the methyl radical. A better estimate is probably to take the average of the entropy effects in reactions 7 and 14, which is −6.5 kcal/mol. This is admittedly a rather uncertain estimate which will affect the estimated barrier quantitatively, but the accuracy of this estimate does not affect the qualitative aspect of the mechanism for methane formation, which is the main goal of the present study. It should also be remembered that the inherent uncertainty of the B3LYP method itself is of the same size as these effects, 3−5 kcal/mol (see section II). With these estimates, −2.6 kcal/mol for zero-point and −6.5 kcal/mol for entropy, the estimated energy to release a methyl radical is lowered from 25.9 kcal/mol down to 16.8 kcal/mol.

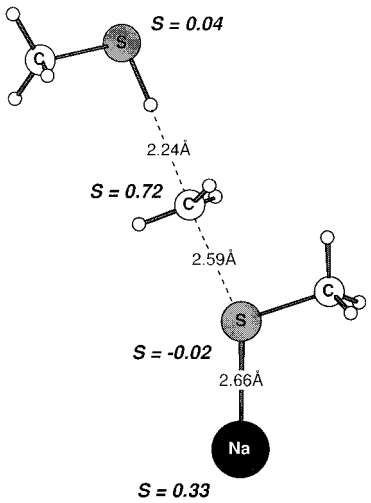

Figure 5. Optimized transition state for the model reaction in which a Na atom replaces the nickel cofactor of MCR (see eq 14 for the overall reaction). The unpaired spin populations are shown in the figure.

From the above results, a mechanism in which a methyl radical is created in the first step appears quite possible. However, a requirement for this to be possible is that the subsequent reaction between the methyl radical and cofactor B to form methane does not lead to an additional large barrier. The calculations for reaction 15:

$$CH_3-S-H + \bullet CH_3 \rightarrow CH_3-S\bullet + CH_4 \quad (15)$$

where cofactor B is modeled by CH_3-S-H, leads to a very small barrier of 1.0 kcal/mol and an exothermicity of 19.3 kcal/mol, with zero-point effect of 3.5 kcal/mol and entropy effect of 0.5 kcal/mol included. Together with the energy to release a free methyl, these values lead to an estimated exothermicity of 2.5 (= 19.3 − 16.8) kcal/mol and an estimated barrier of 17.8 (= 16.8 + 1.0) kcal/mol. It is thus already clear that this type of mechanism appears energetically feasible.

The present mechanism thus consists of two steps, the first one is the formation of the methyl radical, and the second one is the formation of the methane molecule via a hydrogen-atom abstraction from cofactor B. A natural question then is whether a concerted transfer of methyl from coenzyme M to cofactor B to form methane could lead to a still lower barrier? To investigate the possibility for a concerted transition state, the simple model mentioned above for reaction 14 was used. In this model reaction the entire cofactor F_{430} is replaced by a sodium atom, while CoM and CoB are both modeled as simply as possible. This led to a transition state shown in Figure 5

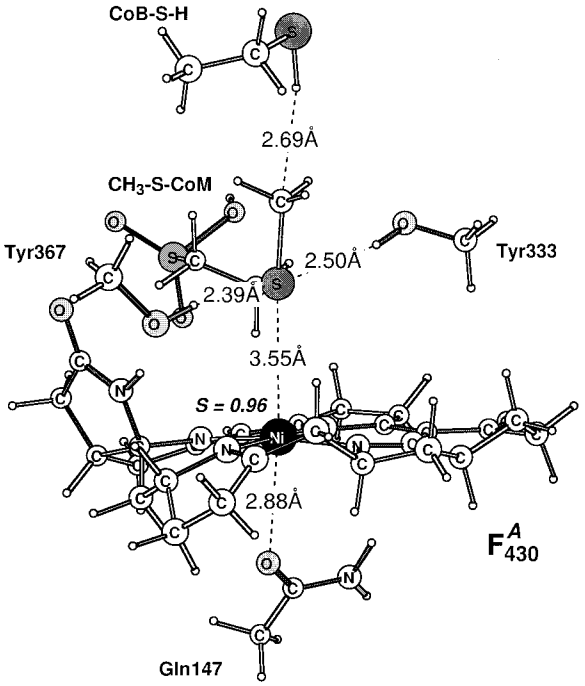

Figure 6. Optimized structure for the initial reactant complex including coenzymes methyl-CoM and CoB.

with a barrier of 13.8 kcal/mol (including zero-point and entropy effects) and with an imaginary frequency of 312 cm^{-1}. The binding energy of the methyl radical in this system can be obtained from reaction 16:

$$CH_3-S-CH_3 + Na \rightarrow \bullet CH_3 + CH_3-S-Na \qquad (16)$$

and was found to be 12.5 kcal/mol. This means that the barrier height for reaction 14 (13.8 kcal/mol) is very close to the sum of the calculated barrier for reaction 15 (1.0 kcal/mol) and the energy for releasing the methyl radical according to reaction 16 (12.5 kcal/mol), showing that methyl is essentially a free radical at the transition state. The possibility of simultaneously breaking the $S-CH_3$ bond and forming the $H-CH_3$ bond thus hardly lowers the barrier. This picture is confirmed by both the spin populations at the transition state (see Figure 5), with a spin of 0.72 for methyl, and by the planar geometry of the methyl group.

One of the most interesting results of the simple model calculations using a sodium atom is the S···S distance at the transition state of 6.24 Å. As mentioned above, the very long S···S distance of 6.2 Å between the cofactors in the X-ray structure is one of the most surprising features of the structure. From this simple model calculation it thus turns out that this long distance is actually optimal for transfer of an essentially free methyl radical, which is another indication that this type of mechanism could indeed be the one used by the enzyme.

III.d. The Large Model Calculations. The above estimates of key bond energies suggest a mechanism for methane formation in which a methyl radical is first formed and then takes a hydrogen atom from CoB to form methane. To test this mechanism, a larger model including all components at once was finally used. The structure of the reactant using this larger model, composed of 107 atoms, is shown in Figure 6. The large F^A_{430} model is used for the F_{430} cofactor, the full model for CoM, while for CoB an ethanethiol is used. The axial glutamine ligand on nickel is modeled by an acetamide and the two tyrosines by methanols. To stay reasonably close to the X-ray structure a few interatomic distances were frozen from this structure. The distances between the terminal methyl carbon of the ethanethiol CoB model and four nuclear centers of the F^A_{430} were frozen during the geometry optimization to the values found in the 1MRO PDB file.[9] The F_{430} centers most naturally frozen are the four carbons of the A, B, C, and D pyrrole rings, which link the F_{430} cofactor to the body of the enzyme via acetate substituents, see Figure 1. The CoB heptanoyl arm with its terminal thiol group is generally expected to bind quite firmly in the pocket, which is critical for the reaction due to the large distance between the thiol sulfur and F_{430} region. Therefore, it was found necessary to fix this group in our model calculations to reproduce some of the rigidity of the MCR active site. Similarly, the terminal methyl carbon of the acetamide model for the Gln147 axial ligand was constrained to maintain the distances to the four F_{430} carbons frozen during the optimization procedure. The approximation of terminal freezing has been applied recently in the theoretical study of the hydrolysis by thermolysin.[25] The two extreme cases for treating strain from the surrounding protein, the completely relaxed and the terminal freezing models, gave only small energetic differences. For example, a calculated activation energy changed by 1.3 kcal/mol only.

The optimized structure has the expected general features. The distance between Ni(I) and the thioether sulfur in CoM is quite long, 3.55 Å, indicative of a very weak Ni−S bond energy. Instead, CoM is held in place by many weak hydrogen bonds to the tetrapyrrole part of F_{430}. There are also hydrogen bonds to the tyrosines. The distance between the methyl group of methyl-CoM and the hydrogen atom of CoB, which will eventually combine to form methane, is also quite long at 2.69 Å.

A structure close to the transition state for methane formation is shown in Figure 7. Since the model is too large for making a full transition state optimization, an approximate transition state was obtained by freezing the distance between the sulfur of CoM and the methyl group to different values around 2.60 Å, which was the fully optimized value for the smaller Na model, see Figure 5. The transition state is taken as the maximum on this one-dimensional potential energy surface, and using a parabolic fit this gives a sulfur-to-carbon distance of 2.67 Å. The very small shift in the sulfur-to-carbon distance as compared to the fully optimized transition state for the small model, together with the small energy change, 0.4 kcal/mol between the calculated point with 2.60 Å and the fitted maximum, indicates that the approximate transition state should be accurate enough. The free character of the methyl radical is seen in the figure by the long optimized distance of 2.57 Å to the hydrogen atom of CoB. The spin on methyl is 0.76. It should be noted that the energy actually goes down by as much as about 3 kcal/mol when the sulfur−carbon distance is increased beyond the approximate transition state to a value of 2.9 Å, at the same time as the proton stays close to the cofactor B sulfur. It is therefore again concluded that the formation of methane is a two-step process in which a free methyl is first released. Since the barrier of the second step, the actual methane formation,

(25) Pelmenschikov, V.; Blomberg, M. R. A.; Siegbahn, P. E. M. *J. Biol. Inorg. Chem.* **2001**, published online.

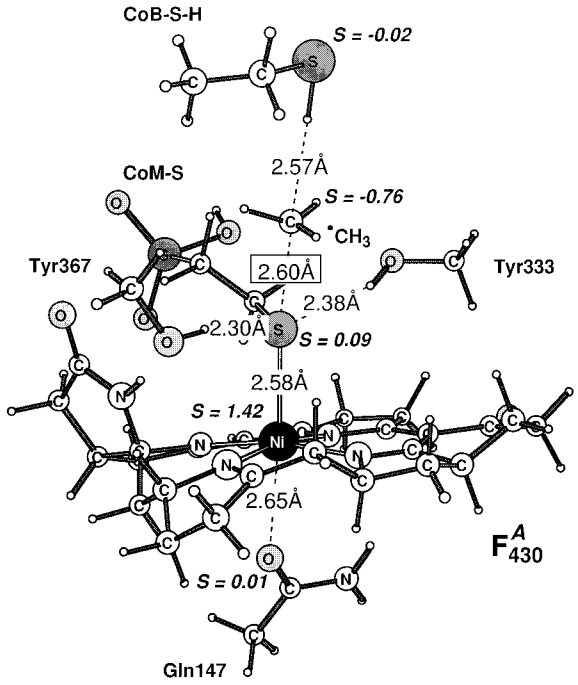

Figure 7. Optimized structure close to the transition state for methane formation. The sulfur−carbon distance in methyl-CoM thioether, chosen as a reaction coordinate, was found to be 2.67 Å at the actual transition state. Selected spin populations are given for the Ni center, the CoB and CoM sulfurs, the methyl carbon and the Gln147 oxygen.

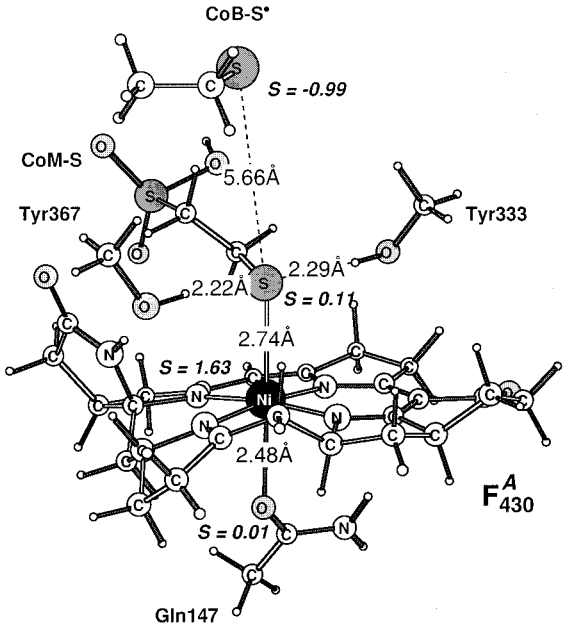

Figure 8. Optimized structure for the intermediate in the mechanism proposed here for MCR. A weakly bound methane molecule formed at this stage was excluded from the system. Selected spin populations are given for the Ni center, CoB and CoM sulfurs and Gln147 oxygen.

was found to be very low (around 1 kcal/mol), the first step should be rate-limiting. The computed barrier is 28.3 kcal/mol using the large basis, only slightly higher than the above estimates (25.9 + 1.0 kcal/mol). With the addition of the zero-point (−2.6 kcal/mol) and entropy effects (−6.5 kcal/mol) obtained from the Na-reaction, the free energy barrier becomes 19.2 kcal/mol. Dielectric effects from the surrounding protein, computed by Jaguar as described in section II, slightly increase this value by 0.3 kcal/mol, leading to the best present estimate of 19.5 kcal/mol for the free energy barrier. Further structural parameters of interest are the S−H hydrogen-bonding distances to the tyrosines, which become smaller as compared to the reactant complex (2.38 vs 2.50 Å for Tyr333, and 2.30 vs 2.39 Å for Tyr367), indicating some transition state stabilization, and a rather long Ni−O distance to Gln147, which does not indicate a significant role for this residue in this part of the mechanism. The effect of Gln147 was not further investigated, but it can be pointed out that a larger model and a larger basis set might change the Ni−O distance slightly.

To obtain quantitative estimates of the different energetic contributions in the methane formation reaction, parts were removed stepwise from the large model, keeping the rest of the structures unchanged from the fully optimized ones. First, removing cofactor B from the model has almost no effect on the energy difference between the structures, again showing that the methane reaction is not concerted. Second, if the tyrosines are also removed from the model, the barrier increases by 5.5 kcal/mol. This value is reasonably similar to the estimate of 6.6 kcal/mol given in the previous section. These values indicate a significant role of the tyrosines, and this effect alone would explain why these residues are conserved for MCR. It should be noted that the effect of the tyrosines might be slightly smaller, since density functional theory tends to overestimate the strength of hydrogen bonds. However, this is mainly a structural problem, giving too short bond lengths, while the relative energies are expected to have very small errors when large basis sets and hybrid functionals are used, as in the present case. Third, replacing the full methyl−CoM model by the small CH_3-S-CH_3 model, has only a small effect of 1.1 kcal/mol on the barrier, actually decreasing it. Apparently, the detailed structure of cofactor M has not been selected to reduce the barrier for methane formation, but there must be other structural reasons for it. Finally, the difference between the large and the small model for F_{430} was estimated by replacing the large F_{430}^{A} with the smaller F_{430}^{B} model and reoptimizing. Cofactor B and the tyrosines were left out, and the smallest model of cofactor M was used. This calculation showed a very small difference of only 0.6 kcal/mol between the models. Therefore, the specific details of the pyrroles and of ring substituents were not selected to decrease the barrier for methane formation either.

The optimized structure of the intermediate product of the methane formation step is shown in Figure 8. The methane molecule was left out from the model. For this structure, zero-point (3.5 kcal/mol) and entropy (0.5 kcal/mol) contributions were calculated relative to the transition state and approximated from reaction 15. With the inclusion also of dielectric effects of −2.4 kcal/mol, the methane formation in MCR is found to be exothermic by 1.8 kcal/mol.

The presently proposed mechanism for MCR is summarized in Figure 9. The reaction starts with the active Ni(I) state of the F_{430} cofactor and with CoM and CoB in place with a long distance of 5.9 Å between the sulfurs. A methyl radical is then released in the key step of the reaction with an estimated barrier of 19.5 kcal/mol. At the same time, Ni(II) forms a fairly strong bond of 38.6 kcal/mol to the sulfur of CoM, step (17):

$$\mathrm{CoB-S-H + CH_3-S-CoM + Ni(I)F_{430} \rightarrow CoB-S-H + {\bullet}CH_3 + CoM-S-Ni(II)F_{430}} \quad (17)$$

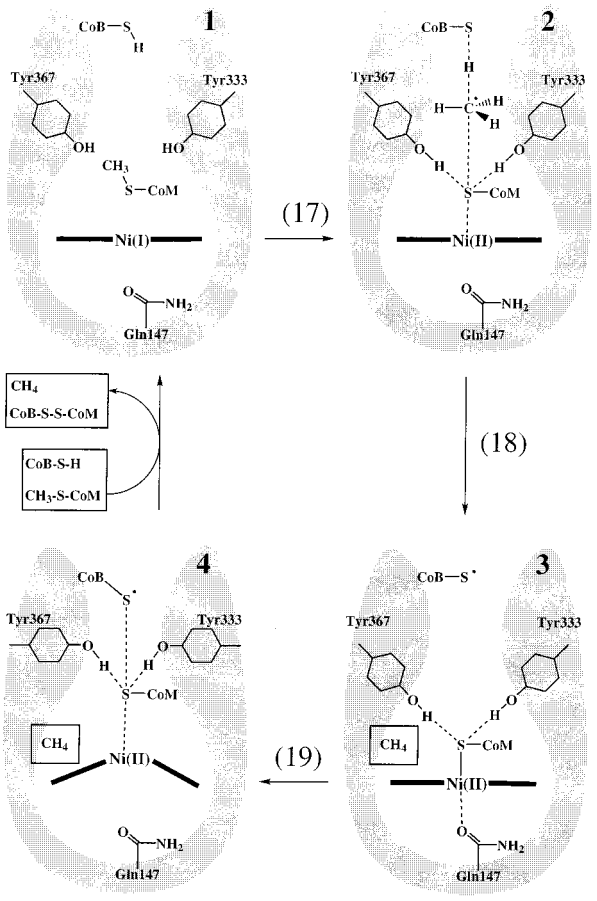

Figure 9. Catalytical mechanism proposed for methane formation in methanogens (see eqs 17−19 for the details).

The methyl radical then abstracts the hydrogen atom from CoB forming methane and the CoB radical, leading to stereoinversion at the carbon, step (18):

$$\mathrm{CoB{-}S{-}H + {\bullet}CH_3 + CoM{-}S{-}Ni(II)F_{430} \rightarrow CoB{-}S{\bullet} + CH_4 + CoM{-}S{-}Ni(II)F_{430}} \quad (18)$$

In the final step 19, the S−S bond between the cofactors is formed:

$$\mathrm{CoB{-}S{\bullet} + CoM{-}S{-}Ni(II)F_{430} \rightarrow CoB{-}S{-}S{-}CoM + Ni(I)F_{430}} \quad (19)$$

Since CoB is firmly bound to the polypeptide by hydrogen bonds and CoM is strongly bound to nickel, this reaction requires a distortion of the F_{430} cofactor in view of the large distance of 5.66 Å between the sulfurs of CoB and CoM (see Figure 8 and point **4** in Figure 9). This part of the mechanism is still under investigation, but the barrier appears to be fairly small.

One implication of the present work is that $CH_3{-}S{-}CoM$ cannot bind prematurely to Ni(I) because that would lead to liberation of a $\bullet CH_3$ radical. Even though endothermic by 20 kcal/mol at room temperature, this could occur with a nonnegligible rate, considering that some of the organisms involved have growth temperature optima as high as 98 °C. In the absence of CoB to quench it, this radical could destroy the surrounding polypeptide by H-atom abstraction. For efficient operation therefore, the enzyme is expected to incorporate a safety device to prevent such premature release. The fact that CoM has a sulfonate group, combined with the fact that the active site pit is both long and has nonpolar walls, may be enough to prevent CoM from binding productively to Ni(I) before CoB is present. CoM could still bind, however, for example at the mouth of the pit, where salt bridges could form to surface residues, just as they do to the phosphothreonine of CoB in the active form. With the arrival of CoB, the affinity of the hexamethylene chain for the nonpolar pit could displace the CoM from its nonproductive binding site and cause it to descend the pit under the impulse of CoB, much as a piston can compress gas in a cylinder. This would guarantee that the methyl radical would immediately find the thiol group of CoB when released by contact with Ni(I), because CoB is the piston that brings CoM into contact with Ni(I). It should be added that the methyl radical is potentially much more dangerous for the enzyme than the CoB−S• radical, which is also present in the suggested mechanism. The main reason for this is that the methyl radical can move much more freely in the enzyme than the CoB radical. Their reactivity should otherwise be rather similar, since one should remember that the CoB radical is suggested to be an intermediate, while the methyl radical is only a relatively high transition state and does therefore not persist.

This is just one scenario of many possible but related ones. The essential point is that CoM is expected only to bind nonproductively (i.e., not to Ni) until CoB has descended the pit and is ready to quench the methyl radical. This explains the great sensitivity of the chemistry to the length of the methylene chain in CoB. As mentioned previously, activity is almost or completely abolished if the chain length is altered by a single methylene group. The chain length of CoB should also be important for the second step of S−S bond formation. The mechanism, where an S···S distance of 6.2 Å is optimal for methyl release, also explains the sensitivity of the system to the nature of the terminal group on the CoM, methyl and ethyl but not propyl being active. The propyl compound is even an inhibitor.[27]

Another factor that is at least consistent with the present proposal is the presence of four methylated amino acids (1-*N*-methylhistidine, *S*-methylcysteine, 5-*S*-methylarginine, and 2-*S*-methylglutamine) in the vicinity of the active site. The majority of these modifications are conserved in several species, suggesting they have a definite role. The methylation does not come from methyl radical release during the methanogenesis mechanism, however, but probably by posttranslational enzymatic methylation.[28] These modifications are expected to make the residues in question more resistant to H-atom abstraction by methyl radical and also more nonpolar; both factors would be favorable to the smooth operation of MCR.

III.e. Stereoinversion at the Reactive Carbon. The suggested mechanism in Figure 9 is in line with experimental data which indicate that an inversion of configuration at the reactive carbon occurs on reduction, a result obtained using an isotopically chiral form of ethyl-coenzyme M, $CH_3CH_2{-}S{-}CoM$.[26] Taken with the results reported here, this inversion implies that the radical is almost immediately quenched by the CoB thiol and does not have the time or the space to rotate in the pit.

(26) Ahn, Y.; Krzycki, J. A.; Floss, H. G. *J. Am. Chem. Soc.* **1991**, *113*, 4700.
(27) Gunsalus, R. P.; Wolfe, R. S. *J. Biol. Chem.* **1978**, *255*, 1891.
(28) Grabarse, W.; Mahlert, F.; Shima, S.; Thauer, R. K. *J. Mol. Biol.* **2000**, *303*, 329.

This suggests that CoB is already in near contact with the methyl of the $CH_3-S-CoM$ before the $S-CH_3$ bond cleaves.

According to the experimental data on fluoromethyl derivatives of the coenzyme M, relevant as MCR substrate analogues, difluoromethyl-coenzyme M ($CHF_2-S-CoM$) was reduced by the enzyme, but trifluoromethyl-coenzyme M ($CF_3-S-CoM$) was totally inactive, even an inhibitor. Differences in the S−C bond strengths do not explain these results, since the calculations show that the S−C bond strengths are approximately equal for the different substrates, within a few tenths of a kcal/mol. Interestingly, the major qualitative difference found in the present work between $CHF_2-S-CoM$ and $CF_3-S-CoM$ is the stereoinversion barrier of the respective radicals, arising from attack of Ni on sulfur. For $\bullet CF_3$, a stereoinversion barrier of 24.3 kcal/mol was obtained, as compared to the value of only 6.1 kcal/mol for $\bullet CHF_2$. In the case of the natural substrate, methyl-coenzyme M, the stereoinversion barrier is obviously equal to zero, since the methyl radical is planar. Again, these results suggest that the radical, once released, should be immediately quenched by CoB, and probably has no possibility to rotate in the pit, otherwise $CF_3-S-CoM$ would also be active as a substrate. It should be added that the transition state for the C−H bond-formation in MCR for these substrates does not necessarily have to be at the top of the barrier for inversion, but it is clear that the barrier for stereoinversion should enter in some way.

III.f. Conformations and Electronic Structure of F_{430} in Different States. The F_{430} porphyrinoid macrocycle has been the subject of numerous investigations, both in its isolated form and as a component of the MCR active site. Debates on the correct interpretation of recent EPR and ENDOR spectroscopic data[29,30] have made a quantum chemical analysis[31,32] of F_{430}-like complexes in Ni(I), Ni(II), and Ni(III) oxidation states attractive as a complement to the experimental proposals. In this section some details concerning the geometry and the electronic properties of F_{430} are reported. For both the F^A_{430} and the F^B_{430} model, the coordination of the Ni(I) reactant was found to be square planar, while the $CoM-S-Ni(II)F_{430}$ adduct was found to have an octahedral coordination around the Ni(II) core.

As discussed above, the F^A_{430} and F^B_{430} models of the tetrapyrrole cofactor give extremely similar results in terms of the bond strengths between the metal and the methyl or CoM sulfur axial ligands. It is therefore not surprising that a high degree of similarity between the two models is found also for the electronic and geometric structures as revealed by the population analysis and the Ni−N distances reported in Tables 1, 2, and 3. Thus, the key electronic properties of the Ni center in the MCR active site can be satisfactorily modeled by retaining solely the very nearest surrounding of the metal atom, that is, by the square planar framework of the four nitrogens, denoted N_A, N_B, N_C, and N_D, depending on which pyrrole ring they belong to, see Figure 4. The weak conjugation in the F_{430} cofactor is a likely explanation for this insensitivity to the size of the model.

An interesting result concerning the Ni−N framework in F_{430} is that the Ni−N bond distances span an unusually broad range as has been discussed previously,[32] see Table 3. In comparison, EXAFS data indicate at least two sets of Ni−N distances. For $Ni(I)F_{430}$ EXAFS gave distances of 1.90 and 2.04 Å, with the assumption of two different Ni−N bond distances in equal proportion. The presently optimized $Ni-N_A$ distance of 2.23 Å in $Ni(I)F^A_{430}$ is thus somewhat long. In a previous quantum chemical study of F_{430}[32] the $Ni(I)-N_A$ distance was found to be 2.14 Å, using similar methods as in the present study but with slightly larger basis sets in the geometry optimization. It should be noted that the potential surface for the Ni−N distances is expected to be quite flat, which means that the energy is quite insensitive to these distances. Single-shell EXAFS fits for the $Ni(II)F_{430}$ high-spin $S = 1$ species in water resulted in an average Ni−N distance of 2.10 Å, quite well correlated to our corresponding value of 2.08 Å for the $CoM-S-Ni(II)F^A_{430}$ complex. Furthermore, in the crystal structure of the Ni(II) $MCR_{ox1-silent}$ form of the enzyme the Ni−N distances vary between 1.99 and 2.14 Å, with the longest value for N_A,[9] in reasonable agreement with the present results for the Ni(II) species.

Table 1. Selected Mulliken Spin Populations for the F_{430} Cofactor and Its Axial Ligands in the Free $Ni(I)F_{430}$ and the $CoM-S-Ni(II)F_{430}$ Complexes, Using the F^A_{430}/F^B_{430} Models

	$Ni(I)F_{430}$	$CoM-S-Ni(II)F_{430}$
	F_{430}	
Ni	0.96/0.96	1.63/1.62
N_A	0.02/0.03	0.06/0.05
N_B	0.04/0.04	0.06/0.06
N_C	0.05/0.05	0.07/0.06
N_D	0.04/0.04	0.07/0.07
	Axial Ligands	
CoM−S	−/−[a]	0.11/0.13
O_{Gln147}	−/−[a]	0.01/0.02

[a] No axial ligand binding for the free $Ni(I)F_{430}$ complex.

Table 2. Selected Mulliken Charge Populations for the F_{430} Cofactor and Its Axial Ligands in the Free $Ni(I)F_{430}$ and $CoM-S-Ni(II)F_{430}$ Complexes, Using the F^A_{430}/F^B_{430} Models

	$Ni(I)F_{430}$	$CoM-S-Ni(II)F_{430}$
	F_{430}	
Ni	0.43/0.32	0.67/0.53
N_A	−0.36/−0.33	−0.37/−0.33
N_B	−0.43/−0.45	−0.43/−0.40
N_C	−0.46/−0.47	−0.48/−0.49
N_D	−0.44/−0.44	−0.43/−0.41
	Axial Ligands	
CoM−S	−/−[a]	−0.49/−0.47
O_{Gln147}	−/−[a]	−0.40/−0.37

[a] No axial ligand binding for the free $Ni(I)F_{430}$ complex.

Table 3. Ni−N Interatomic Distances (Å) in the F_{430} Cofactor for the Free $Ni(I)F_{430}$ and $CoM-S-Ni(II)F_{430}$ Complexes, Using the F^A_{430}/F^B_{430} Models

	$Ni(I)F_{430}$	$CoM-S-Ni(II)F_{430}$
$Ni-N_A$	2.23/2.20	2.13/2.21
$Ni-N_B$	2.04/2.03	2.07/2.13
$Ni-N_C$	2.09/2.10	2.08/2.15
$Ni-N_D$	2.04/2.02	2.05/2.09

IV. Conclusions

The mechanism for methane formation in MCR has been studied using hybrid density functional methods and a large chemical model consisting of 107 atoms. This model includes

(29) Telser, J.; Horng, Y. C.; Becker, D. F.; Hoffman, B. M.; Ragsdale, S. W. *J. Am. Chem. Soc.* **2000**, *122*, 182.
(30) Telser, J.; Fann, Y.-C.; Renner, M. W.; Fajer, J.; Wang, S.; Zhang, H.; Scott, R. A.; Hoffman, B. M. *J. Am. Chem. Soc.* **1997**, *119*, 733.
(31) Wondimagegn, T.; Ghosh, A. *J. Am. Chem. Soc.* **2001**, *123*, 1543.
(32) Wondimagegn, T.; Ghosh, A. *J. Am. Chem. Soc.* **2000**, *122*, 6375.

all three cofactors, F_{430}, CoM, and CoB, in a realistic way and also has models for the essential hydrogen-bonding tyrosines Tyr333 and Tyr367 at the active site. In a preliminary investigation of relevant bond strengths it was found that the Ni−CH_3 bond was unexpectedly weak for both Ni(II) and Ni(III). In fact, the main mechanisms suggested previously, which require rather strong Ni−CH_3 bonds could already be considered very unlikely at that stage. Instead a mechanism is suggested where the methyl is transferred directly between the cofactors. A fully optimized transition state for methane formation using a quite simple model, with a Na atom instead of the F_{430} cofactor, shows that an S···S distance of 6.2 Å is actually optimal for this reaction and this is precisely the experimental distance between the sulfurs of the CoB and CoM cofactors in the MCR enzyme. Surprisingly, the model calculations further show that the methyl being transferred is best regarded as a free methyl radical in the transition state region, having a large spin and long distances to the sulfurs. The largest model leads to a predicted barrier of 19.5 kcal/mol, which includes substantial entropy and zero-point effects which decrease the barrier. The mechanism implies a stereoinversion at the reactive carbon in agreement with experiment. This stereoinversion explains why trifluoromethyl-coenzyme M (CF_3−S−CoM) has been found totally inactive, since the •CF_3 has a very large inversion barrier of 24 kcal/mol. The conserved tyrosines at the active site are shown to form important hydrogen bonds to the sulfur of CoM that reduce the barrier by about 6 kcal/mol. Model comparisons do not indicate any detailed structural features of either F_{430} or CoM that lead to a lowering of the barrier for methane formation.

Acknowledgment. The National Supercomputer Center (NSC) in Linköping is gratefully acknowledged for a generous grant of computer time. We thank Professor R. K. Thauer and Dr. F. Maseras for valuable discussions and helpful suggestions.

JA011664R